

# Sivers effect at HERMES, COMPASS & CLAS12

S. Arnold\*, A. V. Efremov<sup>†</sup>, K. Goeke\*, M. Schlegel\*\* and P. Schweitzer\*

\*Institut für Theoretische Physik II, Ruhr-Universität Bochum, Germany

<sup>†</sup>Joint Institute for Nuclear Research, Dubna, 141980 Russia

\*\*Theory Center, Jefferson Lab, Newport News, VA 23606, USA

**Abstract.** Single spin asymmetries in semi-inclusive deep-inelastic scattering off transversely polarized targets give information on, among other fascinating effects, a pseudo time-reversal odd parton distribution function, the 'Sivers function'. In this proceeding<sup>1</sup> we review the extractions of this function from HERMES and COMPASS data. In particular, the HERMES pion and kaon data suggest significant sea-quarks contributions at  $x \simeq 0.15$  to the Sivers effect. We present a new fit that includes all relevant sea quark distributions and gives a statistically satisfactory overall description of the data, but does not describe ideally the  $K^+$  data from HERMES. We argue that measurements of the pion- and kaon Sivers effect at CLAS12, and COMPASS, will clarify the situation.

**Keywords:** Sivers effect, pions and kaons, sea-quarks

**PACS:** 13.60.Le, 13.60.Hb

## 1. INTRODUCTION

Ever since the first large single spin asymmetries (SSA) were observed in hadron-hadron collisions [1, 2, 3, 4] spin phenomena in QCD became more and more popular. In particular the SSA in semi-inclusive deeply inelastic scattering (SIDIS) from transversely polarized targets have recently been measured at HERMES and COMPASS [5, 6, 7, 8, 9, 10, 11, 12, 13, 14]. SSA in SIDIS with longitudinally polarized leptons or nucleons have been reported at HERMES and the Jefferson Lab [15, 16, 17, 18, 19, 20, 21]. In a partonic picture structure functions in SIDIS and the Drell-Yan (DY) process with small transverse momenta  $P_\perp \ll Q$  of the final state hadron or the lepton pair, respectively, are sensitive to the intrinsic transverse motion of partons [22, 23, 24], see also the review [25]. This means in the case of SIDIS that structure functions can be expressed in terms of convolutions of transverse momentum dependent (TMD) parton distributions and fragmentation functions. Strict factorization formulae for these processes involving an additional soft factor were discussed and established in [26, 27, 28].

In the production of unpolarized hadrons in DIS of an unpolarized lepton beam off a transversely polarized target there are three leading twist spin structure functions, see e.g. [25], which can be distinguished by their azimuthal distributions proportional to  $\sin(\phi + \phi_s)$ ,  $\sin(\phi - \phi_s)$ , and  $\sin(3\phi - \phi_s)$ . Here  $\phi$  denotes the angle between lepton plane and hadron plane in the lab frame while  $\phi_s$  represents the angle of the transverse spin vector with respect to the lepton plane. In the parton model the structure function proportional to  $\sin(\phi + \phi_s)$  ("Collins effect") is expressed in terms of two chirally-odd

---

<sup>1</sup> Talk given at the CLAS 12 RICH Detector Workshop, January 28 - 29, 2008, Jefferson Lab.

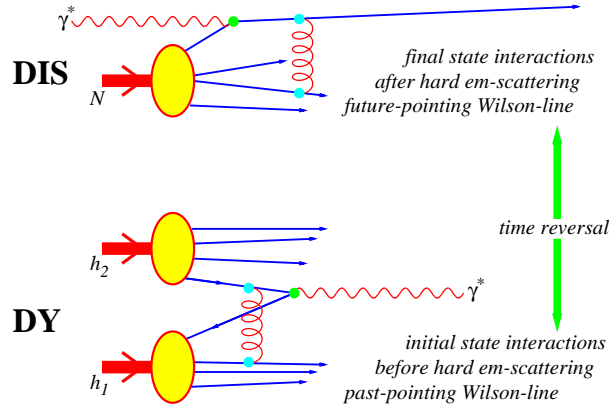


**FIGURE 1.** The SSA due to Sivers effect arises in SIDIS from final state interactions [33] (upper part), and in DY from initial state interactions [34] (lower part). Both types of interactions are encoded appropriately defined Wilson lines that are connected to each other by time reversal [35]. In the Figure the respective interactions are sketched in the one-gluon-exchange approximation, see text.

correlation functions, namely the transversity parton distribution  $h_1^a$  which is not accessible in inclusive DIS, and the Collins fragmentation function  $H_1^\perp$  [29]. The structure function proportional to  $\sin(\phi - \phi_s)$  (“Sivers effect”) is described by the T-odd parton distribution  $f_{1T}^\perp$ , the so-called Sivers function [30, 31], in conjunction with the usual unpolarized fragmentation function  $D_1$ . The structure function proportional to  $\sin(3\phi - \phi_s)$  provides information on the so-called “pretzelosity” distribution  $h_{1T}^\perp$  [23] whose physical interpretation was recently discussed in [32].

T-odd parton distributions such as the Sivers and also Boer-Mulders function  $h_1^\perp$  [24] were considered to vanish due to time-reversal symmetry for some time. Only when it became clear that initial/final state interactions between the struck quark and the target remnants in the parton model can cause SSAs [33, 34], see Fig. 1, the existing definitions of transverse momentum dependent parton distributions were revisited. It was then shown that initial/final state interactions can be implemented into the definitions of parton distributions by means of gauge-link operators with appropriate Wilson lines [35, 36, 37, 38]. In particular these Wilson lines ensure the color gauge invariance of the definition of TMD parton distributions and fragmentation functions. The application of time-reversal switches the direction of the Wilson lines from future-pointing (final state interactions) to past-pointing (initial state interactions) lines in conjunction with an overall sign change. Therefore T-odd parton distributions do not vanish. Instead, time-reversal establishes a connection between T-odd parton distributions in processes with final state interaction (e.g. SIDIS) and in processes with initial state interactions (e.g. Drell-Yan). For the Sivers function the relation reads

$$f_{1T}^\perp(x, \vec{k}_T^2) \Big|_{\text{SIDIS}} = -f_{1T}^\perp(x, \vec{k}_T^2) \Big|_{\text{DY}}. \quad (1)$$

This important QCD-prediction can and still needs to be checked by experiments.

In these proceedings we discuss the present status of the understanding of the Sivers function from HERMES and COMPASS [39, 40, 41, 42, 43, 44, 45, 46, 47]. In particular we review the works [39, 42, 43, 44, 46, 47] and discuss the developments due to the most recent data from SIDIS. We also present predictions for pion and kaon Sivers asymmetries for the 12 GeV upgrade at Jefferson Lab.

## 2. SEMI-INCLUSIVE PROCESSES

In the following we briefly discuss SIDIS with transversely polarized targets, with particular emphasis on the Sivers effect. In SIDIS of an unpolarized lepton beam off a transversely polarized nucleon target one can measure the SSAs [48, 49, 50, 25]

$$\frac{d\sigma^\uparrow - d\sigma^\downarrow}{\frac{1}{2}(d\sigma^\uparrow + d\sigma^\downarrow)} = S_T \left[ \sin(\phi_h - \phi_s) A_{UT}^{\sin(\phi_h - \phi_s)} + \varepsilon \sin(\phi_h + \phi_s) A_{UT}^{\sin(\phi_h + \phi_s)} + \dots \right]. \quad (2)$$

The SSAs  $A_{UT}^{w(\phi, \phi_s)} \equiv F_{UT}^{w(\phi, \phi_s)} / F_{UU}$  are ratios of the respective structure functions to the unpolarized one, which depend on  $x = Q^2 / (2P \cdot q)$ ,  $z = (P \cdot P_h) / (P \cdot q)$ ,  $\vec{P}_{h\perp}^2$  and  $Q^2 = -q^2$  where  $P$  is the target momentum. The angles and other momenta are defined in the left panel of Fig. 2, and  $\varepsilon \sim (1 - y) / (1 - y + y^2/2)$  denotes the polarization of the virtual photon with  $y = (P \cdot q) / (P \cdot l)$ , and  $S_T$  is the transverse spin vector. The dots in Eq. (2) denote terms with other angular distributions due to pretzelosity or subleading twist.

The parton model expressions for the structure functions in terms of convolutions of TMD parton distributions and fragmentation functions can be easily understood when using the "tree-level" formalism of Ref. [23] where only the leading order (in  $\alpha_s$ ) tree diagrams in the hard part are considered. By splitting the SIDIS cross section into a leptonic tensor  $L_{\mu\nu}$  (assuming one-photon exchange) and a hadronic tensor  $W^{\mu\nu}$ ,  $d\sigma_{\text{SIDIS}} \propto L_{\mu\nu} W^{\mu\nu}$ , we can express the leading part (in  $1/Q$ ) of  $W^{\mu\nu}$  by the tree-diagram in the right panel Fig. 2. The lower soft blob in that diagram describes the momentum distribution of quarks inside the target whereas the upper part represents the fragmentation of a parton into hadrons. Field theoretically the soft blobs correspond to

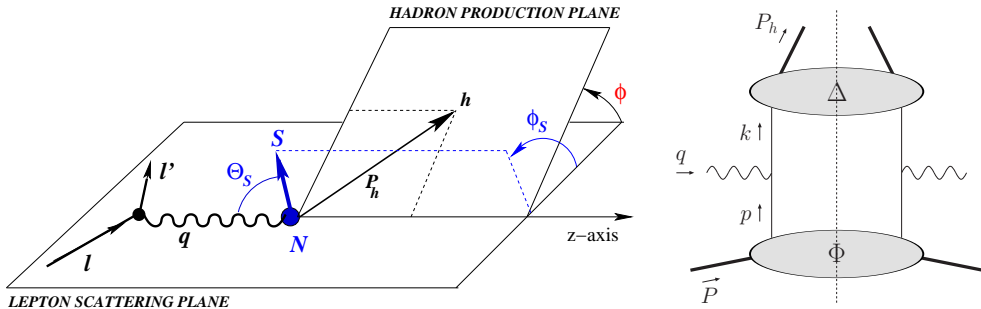


**FIGURE 2.** Left panel: The kinematics of the SIDIS process  $lN \rightarrow l'hX$ . The nucleon is polarized transversely with respect to the beam. However, up to power corrections the polarization is transverse also with respect to the momentum of the virtual photon:  $\sin \Theta_S \sim M_N / Q \ll 1$ . Right panel: Tree-level diagram for the hadronic tensor in leading order in  $1/Q$  in the parton model.

the following matrix elements of bilocal quark-quark operators,

$$\Phi_{ij}(x, \vec{p}_T^2 | \eta) = \int \frac{dz^- d^2 z_T}{(2\pi)^3} e^{ip \cdot z} \langle P, S | \bar{\psi}_j(0) \mathcal{W}_\Phi(0, z | \eta) \psi_i(z) | P, S \rangle \Big|_{z^+ = 0}, \quad (3)$$

$$\Delta_{ij}(z, \vec{k}_T^2 | \eta) = \frac{1}{2z} \sum_X \int \frac{dz^+ d^2 z_T}{(2\pi)^3} e^{ik \cdot z} \langle 0 | \mathcal{W}_\Delta[\infty, z | \eta] \psi_i(z) | P_h, X \rangle \times \langle P_h, X | \bar{\psi}_j(0) \mathcal{W}_\Delta[0, \infty | \eta] | 0 \rangle \Big|_{z^- = 0}. \quad (4)$$

The gauge link operators  $\mathcal{W}_\Phi$  and  $\mathcal{W}_\Delta$  in Eqs. (3) and (4) ensure the color gauge invariance of the matrix elements. They are defined as

$$\mathcal{W}_\Phi[0, (z^-, 0, \vec{z}_T) | \eta] \equiv [0 | a_\Phi] \times [a_\Phi | b_\Phi] \times [b_\Phi | c_\Phi] \times [c_\Phi | (z^-, 0, \vec{z}_T)], \quad (5)$$

$$\mathcal{W}_\Delta[\infty, (0, z^+, \vec{z}_T) | \eta] \equiv [b_\Delta | c_\Delta] \times [c_\Delta | (0, z^+, \vec{z}_T)], \quad (6)$$

$$\mathcal{W}_\Delta[0, \infty | \eta] \equiv [0 | a_\Delta] \times [a_\Delta | b_\Delta], \quad (7)$$

where  $[a|b]$  denotes a gauge link operator, i.e. a path-ordered exponential of gluon field operators, with a straight Wilson line between the space-time coordinates  $a$  and  $b$ . The three "milestones" of the Wilson lines in Eqs. (5)-(7) are  $a_\Phi = (\eta_\infty, 0, \vec{0}_T)$ ,  $b_\Phi = (\eta_\infty, 0, \vec{\omega}_T)$  and  $c_\Phi = (\eta_\infty, 0, \vec{z}_T)$  for the correlator  $\Phi$ , while we have  $a_\Delta = (0, \eta_\infty, \vec{0}_T)$ ,  $b_\Delta = (0, \eta_\infty, \vec{\omega}_T)$  and  $c_\Delta = (0, \eta_\infty, \vec{z}_T)$  for the fragmentation correlator  $\Delta$ . Therein we use the usual light cone coordinates for a four vector  $a^\mu = (a^-, a^+, \vec{a}_T)$  with  $a^\pm = \frac{1}{\sqrt{2}}(a^0 \pm a^3)$ . The parameter  $\eta \in \{-1, 1\}$  determines the direction of the Wilson line. As was pointed out in [35] time-reversal transforms a Wilson line with  $\eta = +1$  describing final state interactions, a situation one encounters in SIDIS, into a Wilson line with  $\eta = -1$  describing initial state interaction, e.g. in Drell-Yan. This results in the relation (1) for the Sivers function.

It is convenient to express the diagram in the right panel of Fig. 2 in terms of the correlators (3) and (4) in a frame in which the momentum of the nucleon  $P$  and the momentum of the produced hadron  $P_h$  are collinear. We obtain for the leading part in  $1/Q$  of the hadronic tensor

$$2MW^{\mu\nu} = 2z \sum_q e_q^2 \int d^2 p_T d^2 k_T \delta^{(2)}(\vec{p}_T + \vec{q}_T - \vec{k}_T) \times \text{Tr} \left[ \Phi^q(x, \vec{p}_T) \gamma^\mu \Delta^q(z, \vec{k}_T) \gamma^\nu \right] + \mathcal{O}(1/Q). \quad (8)$$

The quark-quark correlators  $\Phi$  and  $\Delta$  contain all possible spin information of either the probed or fragmenting quark as well as the spin information of the target. It is possible to project out various polarizations of the quarks by tracing the correlators with appropriate Dirac matrices. These traces can be then parameterized in terms of TMD parton distributions and fragmentation functions [23, 24] (for a complete parameterization see [51]). Assuming that the nucleon moves fast in one light cone direction, i.e.  $P^+$  is the large component of the nucleon momentum, we obtain two TMD distributions for unpolarized quarks by tracing  $\Phi$  with  $\gamma^+$ . One is the well-known ordinary PDF for an

unpolarized target  $f_1$  while the other is the Sivers function, describing the distribution of unpolarized quarks in a transversely polarized nucleon ( $\varepsilon_T^{ij} \equiv \varepsilon^{-+ij}$  with  $\varepsilon^{0123} = +1$ )

$$\frac{1}{2} \text{Tr}[\Phi(x, \vec{p}_T) \gamma^+] = f_1(x, \vec{p}_T^2) - \frac{\varepsilon_T^{ij} p_T^i S_T^j}{M} f_{1T}^\perp(x, \vec{p}_T^2). \quad (9)$$

By tracing  $\Phi$  with other Dirac structures we obtain further PDFs. For example, by tracing it with  $i\sigma^{i+}\gamma_5$  we obtain, among others, the transversity distribution  $h_1$  and the so-called 'pretzelosity' distribution  $h_{1T}^\perp$ , etc.

Since here we consider unpolarized hadrons in the final state only, there are only two relevant fragmentation functions, the ordinary fragmentation of unpolarized quarks and the chirally-odd Collins function  $H_1^\perp$  of transversely polarized quarks. Assuming that the produced hadron moves fast in the minus light cone direction, i.e. the large component of  $P_h$  is  $P_h^-$ , we project them out by tracing with  $\gamma^-$  and  $i\sigma^{i-\gamma_5}$ ,

$$\frac{1}{2} \text{Tr}[\Delta(z, \vec{k}_T) \gamma^-] = D_1(z, \vec{k}_T^2) \quad ; \quad \frac{1}{2} \text{Tr}[\Delta(z, \vec{k}_T) i\sigma^{i-}\gamma_5] = -\frac{\varepsilon^{ij} k_T^j}{M_h} H_1^\perp(z, \vec{k}_T^2). \quad (10)$$

At this point one obtains the expression for the structure functions Sivers structure function by inserting the traces of the type (9), (10) into the hadronic tensor (8), boosting into a frame in which the momentum of the nucleon and of the virtual photon are collinear, and contracting with the leptonic tensor  $L_{\mu\nu}$  which yields:

$$\begin{aligned} F_{UT}^{\sin(\phi_h - \phi_s)} &= x \sum_q e_q^2 \int d^2 p_T d^2 k_T \delta^{(2)}(\vec{p}_T - \vec{k}_T - \vec{P}_{h\perp}/z) \\ &\quad \times \left[ -\frac{\vec{h} \cdot \vec{p}_T}{M_h} f_{1T}^{\perp,q}(x, \vec{p}_T^2) D_1^q(z, \vec{k}_T^2) \right], \end{aligned} \quad (11)$$

where  $\vec{h} = \vec{P}_{h\perp}/|\vec{P}_{h\perp}|$  is the normalized transverse momentum of the produced hadron. The unpolarized structure function  $F_{UU}$  is given by (11) with  $(-\vec{h} \cdot \vec{p}_T) f_{1T}^{\perp,q}/M_h \rightarrow f_1^q$ .

We emphasize again that the result (11) is valid for the tree-level hard process. A factorization valid to all orders requires the inclusion of a soft factor [26, 27, 28] in the formula (11) in order to handle soft gluon radiation. Up to now no phenomenological treatment takes this factor into account. We will neglect this factor in the following.

### 3. SSA IN $\mathbf{p}^\uparrow \mathbf{p} \rightarrow \pi \mathbf{X}$

The first information on the Sivers function was obtained from studies [52, 53] of SSAs in  $p^\uparrow p \rightarrow \pi X$  or  $\bar{p}^\uparrow p \rightarrow \pi X$  [3, 4]. Although they originally motivated the introduction of the Sivers effect [30, 31] the theoretical understanding of these processes is more involved compared to SIDIS or DY. Here SSAs can also be generated by twist-3 effects [54, 55, 56, 57, 58], though it was suggested that these could be manifestations of the same effect in different  $k_T$  regions [59, 60, 61]. Moreover, for this processes no factorization proof is formulated in terms of the Sivers effect. Studies of other processes with  $pp$  in the initial state and hadronic final states indicate that it is in general hard to prove factorization in hadronic reactions [59, 62, 63].

## 4. SIVERS EFFECT IN SIDIS: FIRST INSIGHTS

The first information on the Sivers function from SIDIS was obtained in [39] from a study of preliminary HERMES data [64] on the 'weighted' SSA defined as

$$A_{UT}^{P_{h\perp}/M_N \sin(\phi-\phi_S)}(x) \equiv \frac{1}{S_T} \frac{\sum_i \left\langle \frac{P_{h\perp,i}}{M_N} N_i^\uparrow - \frac{P_{h\perp,i}}{M_N} N_i^\downarrow \right\rangle}{\sum_i \left\langle \frac{1}{2}(N_i^\uparrow + N_i^\downarrow) \right\rangle} \quad (12)$$

where  $N_i^{\uparrow(\downarrow)}$  are sums over event counts for the respective transverse target polarization, and  $\langle \dots \rangle$  denotes averaging — here over  $z$  and  $P_{h\perp}$ . The advantage of 'weighted SSAs' is that the integrals in the structure function (11) can be solved exactly [24] yielding

$$A_{UT}^{P_{h\perp}/M_N \sin(\phi-\phi_S)}(x, z) = \frac{2 \int d\vec{P}_{h\perp}^2 \frac{P_{h\perp}}{M_N} F_{UT}^{\sin(\phi-\phi_S)}(x, z, P_{h\perp})}{\int d\vec{P}_{h\perp}^2 F_{UU}(x, z, P_{h\perp})} = \frac{(-2) \sum_a e_a^2 x f_{1T}^{\perp(1)a}(x) D_1^a(z)}{\sum_a e_a^2 x f_1^a(x) D_1^a(z)} \quad (13)$$

where  $f_{1T}^{\perp(1)a}(x) \equiv \int d^2 \vec{p}_T \frac{\vec{p}_T^2}{2M_N^2} f_{1T}^{\perp a}(x, \vec{p}_T^2)$ .

While the weighting is preferable from a theory point of view, it makes data analysis harder. It is difficult to control acceptance effects, and the HERMES Collaboration does not recommend the use of the preliminary data [64]. In 'unweighted SSAs' defined as

$$A_{UT}^{\sin(\phi-\phi_S)}(x) \equiv \frac{1}{S_T} \frac{\sum_i \left\langle N_i^\uparrow - N_i^\downarrow \right\rangle}{\sum_i \left\langle \frac{1}{2}(N_i^\uparrow + N_i^\downarrow) \right\rangle} \quad (14)$$

acceptance effects largely cancel. Therefore such data have been finalized first, and one even is not discouraged to use preliminary data of this type [7, 9, 10]. However, the prize to pay is that now the convolution integrals in (11) can be solved only by resorting to models for the transverse momentum dependence. Here we assume the distributions of transverse parton and hadron momenta in distribution and fragmentation functions to be Gaussian with the corresponding Gaussian widths,  $p_{Siv}^2$  and  $K_{D_1}^2$ , taken to be  $x$ - or  $z$ - and flavor-independent. The Sivers SSA (14) as measured in [5, 6] is then given by [42]

$$A_{UT}^{\sin(\phi-\phi_S)} = \frac{a_G (-2) \sum_a e_a^2 x f_{1T}^{\perp(1)a}(x) D_1^a(z)}{\sum_a e_a^2 x f_1^a(x) D_1^a(z)} \quad \text{with} \quad a_G = \frac{\sqrt{\pi}}{2} \frac{M_N}{\sqrt{p_{Siv}^2 + K_{D_1}^2/z^2}}. \quad (15)$$

In view of the sizeable error bars of the first data it was necessary to minimize the number of fit parameters. For that in [42] effects of sea quarks were neglected. In addition, the prediction from the limit of a large number of colors  $N_c$  in QCD [65], namely

$$f_{1T}^{\perp u}(x, \vec{p}_T^2) = -f_{1T}^{\perp d}(x, \vec{p}_T^2) \quad \text{modulo } 1/N_c \text{ corrections,} \quad (16)$$

was imposed as an exact constraint. Analog relations holds also for antiquarks, and all are valid for  $x$  of the order  $xN_c = \mathcal{O}(N_c^0)$  [65]. The following Ansatz was made and

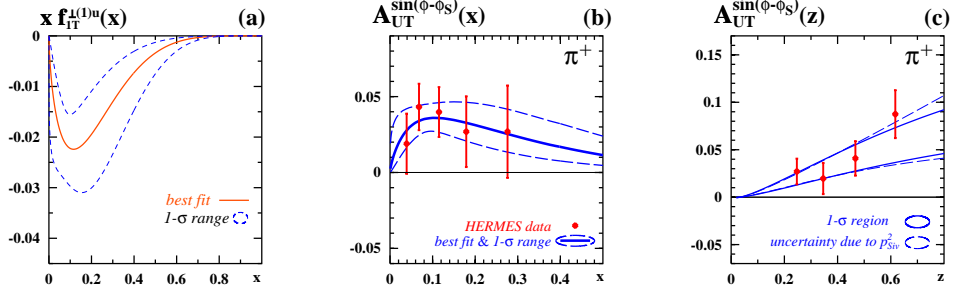


**FIGURE 3.** (a) Sivers function of  $u$ -quarks vs.  $x$  at a scale of  $2.5 \text{ GeV}^2$ , as obtained from HERMES data [5]. Shown are the best fit and its  $1-\sigma$  uncertainty. (b + c) The Sivers SSA, Eqs. (14, 15), for  $\pi^+$  from proton as function of  $x$  and  $z$  as obtained from the fit in Figure 3a in comparison to the data [5]. The  $\pi^-$  data from [5] are compatible with zero, and are equally well described (not shown here).

best fit obtained:  $xf_{1T}^{\perp(1)u}(x) = -xf_{1T}^{\perp(1)d}(x) \stackrel{\text{Ansatz}}{=} Ax^b(1-x)^5 \stackrel{\text{fit}}{=} -0.17x^{0.66}(1-x)^5$  [42, 43]. Fig. 3a shows the fit and its  $1-\sigma$  uncertainty due to the statistical error of the data [5]. Fig. 3b shows that this fit well describes the  $x$ -dependence of the HERMES data [5]. Fig. 3c finally shows the equally good description of the  $z$ -dependence of the data [5], that were not included in the fit. This serves as a cross check for the Gauss Ansatz, which apparently works well here. It is found in general that this model is useful as long as one deals with limited precision and small transverse momenta  $\langle P_{h\perp} \rangle \ll Q$  [66, 53].

In [42] it was furthermore found that effects due to sea quarks could not be resolved within the error bars of the data [5]. It was also checked that  $1/N_c$ -corrections expected in (16) are within the error bars of HERMES [5] and especially COMPASS [8] data.

To draw an intermediate conclusion, the HERMES and COMPASS data [5, 6] are compatible with large- $N_c$  predictions [65]. More precisely, the large- $N_c$  approach worked at that stage, because the precision of the first data [5, 6] was comparable to the theoretical accuracy of the large- $N_c$  relation (16). Remarkably, the signs of the extracted Sivers functions,  $f_{1T}^{\perp u} < 0$  and  $f_{1T}^{\perp d} > 0$ , agree with the physical picture discussed in [67]. The findings of [42] were in agreement with other studies [40, 41], see also the review [45].

## 5. SIVERS EFFECT IN DY: FIRST PREDICTIONS

As the experimental test of the particular 'universality relation' for the Sivers function in Eq. (1) is of fundamental importance, the first insights on  $f_{1T}^{\perp}$  [39, 42] were immediately used to estimate the feasibility of DY-experiments to measure the Sivers effect [39, 42]. It was shown that the Sivers effect leads sizeable SSAs in  $p^{\uparrow}\pi^- \rightarrow l^+l^-X$ , which can be measured at COMPASS, and in  $p^{\uparrow}\bar{p}$  or  $p\bar{p}^{\uparrow} \rightarrow l^+l^-X$ , which could be studied in the proposed PAX experiment at FAIR, GSI [68].

On a shorter term the Sivers effect in DY can be studied in  $p^{\uparrow}p \rightarrow l^+l^-X$  at RHIC. In  $pp$ -collisions sea quarks are involved, and counting rates are smaller. It was shown, however, that the Sivers SSA in DY can nevertheless be measured at RHIC with an accuracy sufficient to unambiguously test Eq. (1) for Sivers quarks [42, 44]. Moreover, RHIC can provide valuable information on Sivers antiquarks [42, 44].

## 6. SIVERS EFFECT IN SIDIS: FURTHER DEVELOPMENTS

The first data [5, 6] gave rise to a certain optimism. The Sivers effect on a proton target was clearly seen [5], its smallness on a deuteron target [6] understood in theory [65]. Independent studies [39, 40, 41, 42] agreed on the interpretation of the SIDIS data [45]. Prospects of accessing the effect in DY (and to test the universality property of  $f_{1T}^\perp$ ) were found promising, see [39, 40, 41, 43] and [69, 70, 71]. The optimism persisted the following releases of higher statistics data [7, 8] from HERMES and COMPASS, but it was somehow damped with the advent of HERMES data on kaon Sivers SSAs [9, 10], while COMPASS reconfirmed that on deuteron the effect is really small [11, 12, 13].

Let us first discuss what one would naively expect for the  $K^+$  Sivers effect. Comparing the 'valence quark structure' ( $K^+ \sim u\bar{s}$  vs.  $\pi^+ \sim u\bar{d}$ ), we see that the DIS-production of  $K^+$  and  $\pi^+$  differs by the 'exchange' of the sea quarks  $\bar{s} \leftrightarrow \bar{d}$ . If it were legitimate to neglect sea quarks in nucleon, then the  $K^+$  and  $\pi^+$  Sivers SSAs would be comparable.

Now let us have a look on the preliminary HERMES data [9]. At larger  $x > 0.15$  the Sivers SSAs for  $K^+$  and  $\pi^+$  are comparable, as expected. The fit to pion data discussed in Sec. 4 well describes the  $K^+$  data in this region [46, 47], see the solid line in Fig. 4a (where, of course, all 'differences' between kaons and pions due to different fragmentation functions [72] are considered). However, at smaller  $x \sim 0.1$  we observe a (2-3) times larger SSA for  $K^+$  compared to  $\pi^+$ . For  $K^- \sim s\bar{u}$  (i.e. pure 'sea quark effect') the SSA is compatible with zero and bears no surprises.

The  $K^+$  Sivers effect at HERMES [9, 10] hints at an importance of Sivers sea quarks. Interestingly, no kaon over pion enhancement is observed at COMPASS [11, 12, 13]. This is remarkable, because the COMPASS kinematics covers much smaller  $x$  down to  $x_{\min} = 0.003$  (vs. HERMES  $x_{\min} = 0.023$ ). Sea quark effects could therefore show up at COMPASS even more clearly — however, one has to keep in mind the different targets: proton at HERMES vs. deuteron at COMPASS.

In order to get a feeling about the impact of sea quark effects, let us do the following exercise. We use for  $f_{1T}^{\perp u}$  and  $f_{1T}^{\perp d}$  the previous best fit results, see Sec. 4, and add on top of that Sivers  $\bar{u}$ ,  $\bar{d}$ ,  $s$  and  $\bar{s}$ -distributions which saturate the positivity bounds [73]

$$|f_{1T}^{\perp(1)a}(x)| \leq \frac{\langle p_T^a \rangle_{\text{unp}}}{2M_N} f_1^a(x) , \quad (17)$$

where  $\langle p_T^a \rangle_{\text{unp}}$  is the mean transverse momentum of unpolarized quarks in the nucleon [42]. (It could depend on flavor. Neglecting this possibility one obtains a good description of transverse hadron momenta at HERMES [17] for  $\langle p_T \rangle_{\text{unp}} = 0.5 \text{ GeV}$  [42].) The effects of sea quarks allowed to saturate  $\pm$  these bounds are shown in Fig. 4a as dashed lines. Throughout the parameterization [74] is used for  $f_1^a$ .

Fig. 4a demonstrates that sea quarks may have a strong impact, and could be able to explain the Sivers  $K^+$  SSA. However, introducing Sivers sea quarks as large as to explain the  $K^+$  data, Fig. 4a, tends to overshoot the  $\pi^+$  data, see Fig. 4b. Also there is no reason to expect Sivers sea quarks to saturate positivity bounds.

If the Sivers  $K^+$  effect is not a statistical fluctuation (which is unlikely, see Fig. 4c), then it should be possible to obtain a satisfactory fit to the pion and kaon data from HERMES and COMPASS. The next Section is devoted to this task.

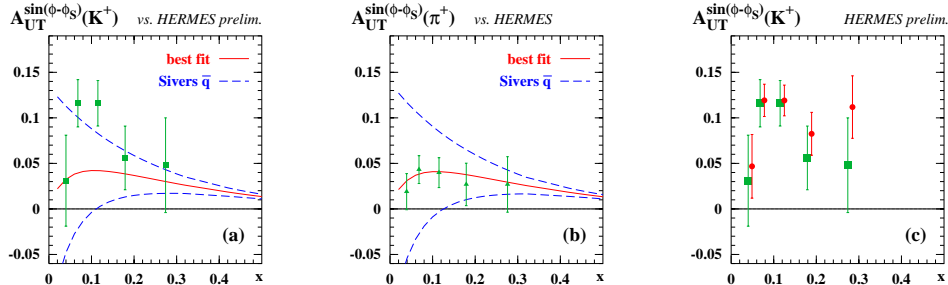


**FIGURE 4.** (a) The Sivers SSA for  $K^+$  as function of  $x$ . The preliminary HERMES data is from [9]. The solid line is the  $K^+$  SSA obtained from the best fit to pion data [5] (see Sec. 4). The dashed lines display the effect of adding on top of that Sivers sea quarks saturating  $\pm$  the positivity bounds (see Sec. 6). It seems that sea quarks could explain the effect, but at the same time one overshoots  $\pi^+$  data (see next figure). (b) Sivers SSA for  $\pi^+$  as function of  $x$ . The published HERMES data are from [5], and the theoretical curves as in Fig. 4b (but for  $\pi^+$ ). (c) Comparison of the first (lower statistics, boxes) [9] and the most recent (higher statistics, circles) [10] data from HERMES on the  $K^+$  Sivers SSA as function of  $x$ . It seems unlikely that the effect could be due to statistical fluctuation, especially in the region of  $x \sim 0.1$ .

## 7. UNDERSTANDING PION AND KAON SIVERS EFFECT

In order to see whether it is possible to understand the data on the Sivers SSAs for pions and kaons from different targets, it is necessary to attempt a simultaneous fit. We use the HERMES proton target data on  $\pi^0, \pi^\pm, K^\pm$  from [10] and the COMPASS deuteron data on  $\pi^\pm, K^\pm$  from [11]. Since we do not know error correlation matrices we cannot perform a simultaneous fit to data on  $x, z$  and  $P_{h\perp}$ -dependences with correct estimate of its statistical significance. In the present study data on  $x$ -dependence will serve as input for the fit, and data on  $z$ -dependence will be used only for a cross check of the results. When using data from different experiments it is necessary to consider systematic uncertainties. Those are dominated by the uncertainty of the target polarization in both experiments, and we combine them with statistical errors in quadrature.

The data on  $x$ -dependences of the Sivers SSAs have little sensitivity to the parameters entering the factor  $a_G$  in (15). We fix the Gaussian width of the fragmentation function and Sivers function as  $\langle K_{D_1}^2 \rangle = 0.16 \text{ GeV}^2$  [42], and  $\langle p_{\text{Siv}}^2 \rangle = 0.2 \text{ GeV}^2$  which coincides with the central value obtained in [42]. We stress that the final results presented here anyway depend only weakly on these parameters, which could be inferred from studies of data on  $P_{h\perp}$ -dependence. Such studies will be reported elsewhere. Finally, for  $f_1^a(x)$  and  $D_1^a(z)$  we use the leading order parameterizations [72, 74] at a scale of  $2.5 \text{ GeV}^2$  which is close to the  $\langle Q^2 \rangle$  of both experiments.

Now we need an Ansatz for the Sivers functions. Here we shall content ourselves to the following simple Ansatz (the constraints on the  $A_a$  arise from positivity, Eq. (17))

$$f_{1T}^{\perp(1)a} = A_a \frac{\langle p_T \rangle_{\text{unp}}}{2M_N} f_1^a(x), \quad |A_a| \leq 1 \quad (18)$$

with  $\langle p_T \rangle_{\text{unp}} = 0.5 \text{ GeV}$  from [42]. Since sea quark effects are of importance (see Sec. 6) we introduce the flavours:  $a = u, d, s, \bar{u}, \bar{d}, \bar{s}$ . So the initial task is to fix the  $N_{\text{para}} = 6$

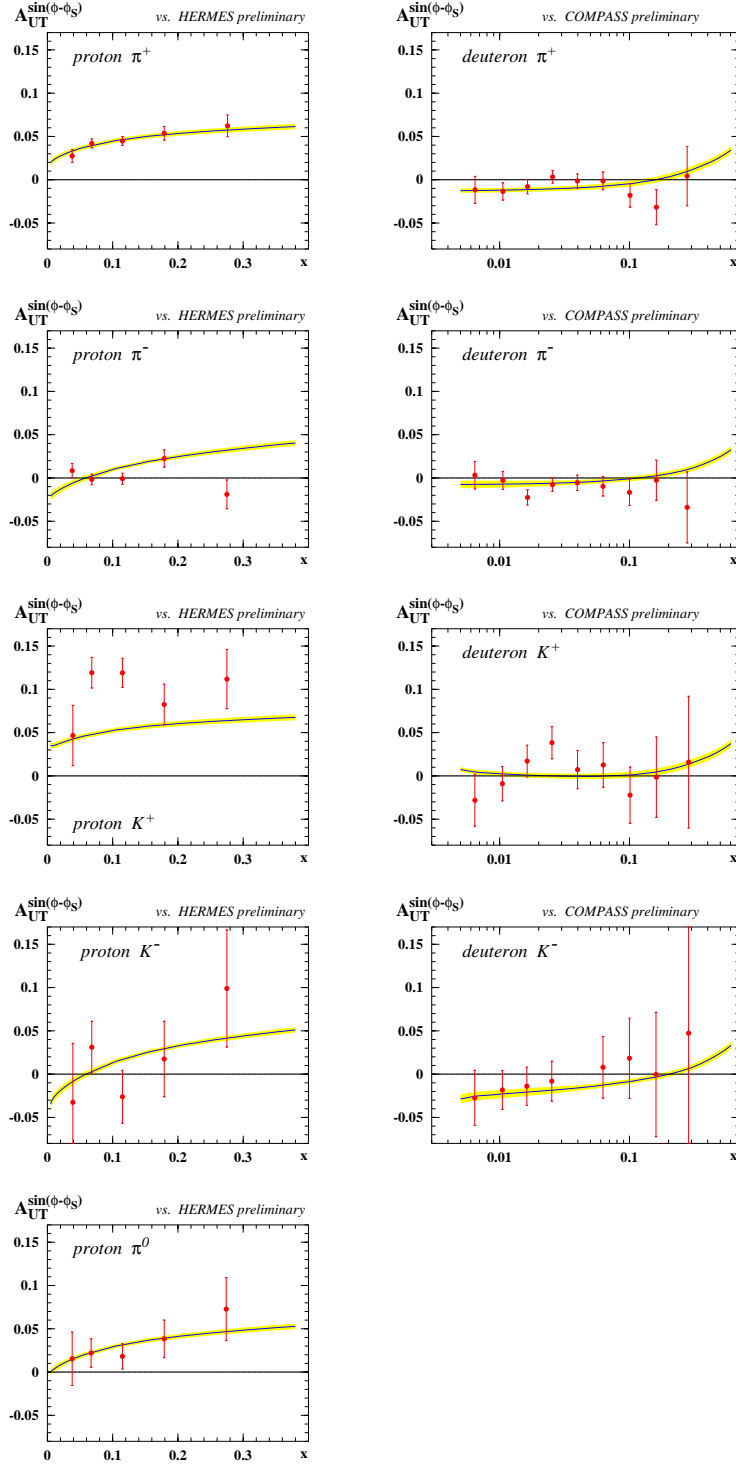


**FIGURE 5.** The Sivers SSA for various hadrons from different targets vs.  $x$ . Left panel: HERMES data (proton target) [10]. Right panel: COMPASS data (deuteron target) [11]. The theoretical curves are the best fit (solid line) and its  $1-\sigma$ -region (shaded area) as obtained from the Ansatz and best fit in Eqs. (18, 19). These data served as INPUT for the fit (18, 19).

parameters  $A_a$  from  $N_{\text{data}} = N_{\text{HERMES}} + N_{\text{COMPASS}} = 25 + 36$  data points. The Ansatz (18) makes the numerical handling of the problem particularly simple. The  $\chi^2$  is a 'six-dimensional parabola' in the space of the  $A_a$ , and the only extremum (global minimum) is easily found by means of simple self-made codes, or `minuit` [75].

The best fit has a  $\chi^2 = 73.4$ . This means a satisfactory  $\chi^2$  per degree of freedom of  $\chi^2/(N_{\text{data}} - N_{\text{para}}) \equiv \chi^2_{\text{d.o.f.}} = 1.33$ . The results for the best fit parameters read:  $A_u = -0.21$ ,  $A_d = 0.41$ ,  $A_{\bar{u}} = 0.24$ ,  $A_{\bar{d}} = -0.27$ ,  $A_s = 0.95$ ,  $A_{\bar{s}} = -1.93$ . The (correlated!)  $1-\sigma$  uncertainties of these fit results are of  $\mathcal{O}(10\%)$ . But  $A_{\bar{s}}$  exceeds the positivity bound (18) and  $A_s$  comes suspiciously close to it, which is driven by the  $K^+$  HERMES data.

We therefore repeat the fit and use the above results to inspire the following Ansatz. We fix  $A_s = +1$  and  $A_{\bar{s}} = -1$  from the very beginning. This 4-parameter-fit has, of course, a slightly higher  $\chi^2 = 76.5$  but nearly the same  $\chi^2_{\text{d.o.f.}} = 1.34$  which means that it is equally good. The best fit parameters read

$$\begin{aligned} A_u &= -0.21 \pm 0.01 & A_{\bar{u}} &= 0.23 \pm 0.02 & A_s &\stackrel{\text{fixed}}{=} +1 \\ A_d &= 0.38 \pm 0.03 & A_{\bar{d}} &= -0.28 \pm 0.04 & A_{\bar{s}} &\stackrel{\text{fixed}}{=} -1. \end{aligned} \quad (19)$$

The  $1-\sigma$  errors are those solutions for the  $A_a$  ( $a = u, d, \bar{u}, \bar{d}$ ) which increase the total  $\chi^2 = 76.5$  by one unit. For our Ansatz this is again particularly simple. For example, the uncertainty of  $A_u$  is found by fixing the other free parameters to their best fit values, and solving a quadratic equation. The  $1-\sigma$  uncertainties in (19) are correlated, of course.

Fig. 5 shows how the fit (18, 19) describes the data on the  $x$ -dependence of the Sivers SSAs (i.e. the input for the fit). Let us comment on the fit:

- The fit quality is satisfactory:  $\chi^2_{\text{d.o.f.}} = 1.3 = \mathcal{O}(1)$  as it should be. (There are stronger criteria for goodness of a fit [76], but we have too few data to apply them.)
- Looking at Fig. 5 we notice: out of 61 data points, there are only two(!) data points that are off the best fit curve in a worthwhile mentioning way.
- From the point of view of statistics, one can comfortably live with such a situation, and wait for new data that will allow to improve the fit.
- But is it not suspicious that those two points, that are off the best fit in a worthwhile mentioning way, are precisely the  $K^+$  HERMES data around  $x \sim 0.1$ ?

The last observation raises the question, whether the  $K^+$  HERMES data around  $x \sim 0.1$  could be a statistical fluctuation. Of course, this possibility cannot be excluded — though one is not inspired to consider such an explanation as convincing, looking back at Fig. 4c.

Let us postpone the discussion of this point for later, and continue with  $z$ -dependence. We did not use these data in the fit. Therefore the results, see Fig. 6, are a prediction of the fit (18, 19), and the assumed Gaussian model for transverse parton momenta. The overall performance of the description is again satisfactory. It is not surprising that the only worthwhile mentioning mismatch is for the  $K^+$  data from HERMES.

At this point, one could try to improve the description of  $z$ -dependence by re-adjusting the parameters  $p_{\text{Siv}}^2$  and  $K_{D_1}^2$  in Eq. (15). In particular,  $K_{D_1}^2$  could even be allowed to be  $z$ -dependent. With different  $p_{\text{Siv}}^2$  and  $K_{D_1}^2$  one would, of course, obtain somehow different  $A_a$  in the best fit (18, 19). This could be continued to an iteration procedure, which (if convergent) would result in a optimized description of data on  $x$ - and  $z$ -dependence.

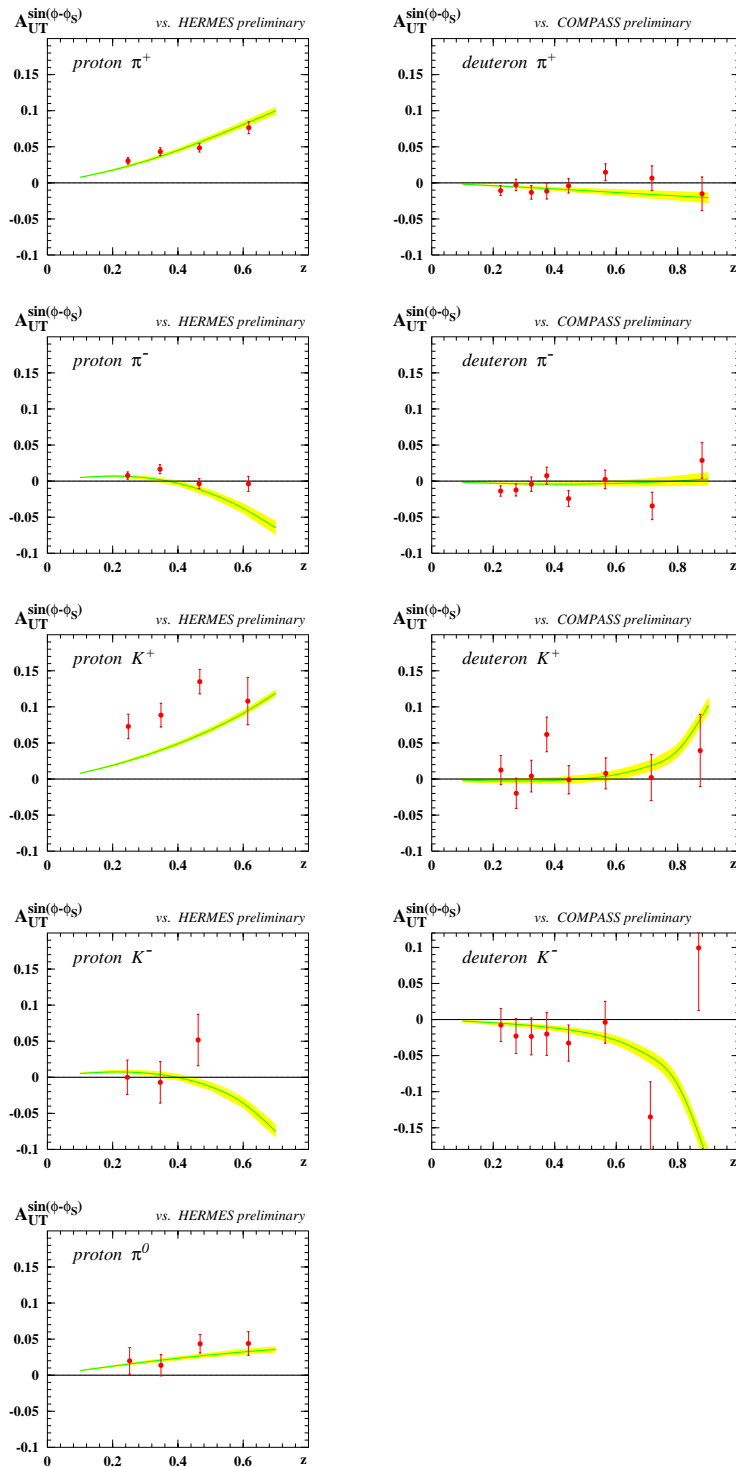


**FIGURE 6.** The Sivers SSA for various hadrons from different targets vs.  $z$ . Left panel: HERMES data (proton target) [10]. Right panel: COMPASS data (deuteron target) [11]. The theoretical curves are the best fit (solid line) and its  $1-\sigma$ -region (shaded area) as obtained from the Ansatz and best fit in Eqs. (18, 19). These results are a PREDICTION of the fit (18, 19).

$P_{h\perp}$ -dependence could also be included. This procedure would help to better constrain the parameters  $p_{\text{Siv}}^2$  and  $K_{D_1}^2$ . But it presumably would have little impact on the fit results (19). Keeping this in mind, we shall — at the present stage of art — content ourselves with the descriptions in Figs. 5 and 6. The  $P_{h\perp}$ -dependence will be discussed elsewhere.

## 8. HOW DOES THE SIVERS FUNCTION LOOK LIKE?

In Sec. 7 we have seen that the probably simplest Ansatz one can imagine for the Sivers function, see Eq. (18), works. 'It works' means in this context that it yields an acceptable  $\chi^2$  per degree of freedom of  $\chi_{\text{d.o.f.}} = \mathcal{O}(1)$ . Other, more flexible Ansätze could yield better descriptions. In particular, it is an interesting question, whether one could better describe the proton target  $K^+$  Sivers effect. Different Ansätze with more free parameters (and the impact of different fragmentation functions) were explored in [77], but a 'better' description of the kaon HERMES data could not be reported there, neither.

However, having achieved a  $\chi_{\text{d.o.f.}} = 1.3$  one must wonder, whether there really is a necessity to improve that fit. Let us adopt here the point of view that it is not, and draw conclusions from our results.

- The Ansatz (18) is rather rigid. It denies the Sivers function an independent  $x$ -shape, and forces it to be proportional to  $f_1^a(x)$ . The only "freedom" it gives to  $f_{1T}^{\perp a}$  is that the proportionality factors  $A_a$  can be flavor dependent. (To recall: we included the factor  $\langle p_T \rangle_{\text{unp}} / (2M_N)$  in (18) such that  $|A_a| \leq 1$  guarantees positivity (17).)
- The initial, unconstrained six-parameter-fit forced the Sivers  $s$  ( $\bar{s}$ ) function to come close to  $(+1) \times$  (to exceed  $(-1) \times$ ) the positivity bound (17).
- Because of that, in the final four-parameter-fit, we fixed the Sivers strangeness functions such that they saturate  $\pm$  the positivity bounds:  $A_s = +1$  and  $A_{\bar{s}} = -1$ .
- One may worry whether such a large 'Sivers strangeness' in the nucleon is natural. However: (i) the 'net Sivers strangeness content' is zero ( $s$ ,  $\bar{s}$  have opposite signs). (ii) Fixing, for example,  $A_s = \frac{1}{2}$  and  $A_{\bar{s}} = -\frac{1}{2}$  (explores positivity only within 50%), would increase the  $\chi^2_{\text{d.o.f.}}$  by only 0.07 units — i.e. an equally acceptable fit. Thus, presently there is no reason to worry about the Sivers strangeness functions. (Moreover  $\langle p_T \rangle_{\text{unp}}$  in (17), defined within the Gauss model approximation, could be flavor-dependent and different for  $s$ ,  $\bar{s}$ , possibly relaxing numerically the bound imposed here.)
- It is a reasonable guess that the Sivers function is suppressed at small  $x$  compared to  $f_1^a(x)$  [41]. But it is not necessary to build in such a suppression in the Ansatz in order to describe the COMPASS data rather precise at small  $x$ . In our fit this is achieved by the different relative signs of the Sivers functions.
- We do not mean that the Sivers function should raise like  $f_1^a(x)$  at small  $x$ . Rather we would like to stress that a suppression of the Sivers function compared to  $f_1^a(x)$ , if existent, is not yet constrained by the present data.
- We can draw from our study even the following stronger conclusion. The present data do not yet tell us much about the shape of the Sivers function. But they tell us something about its magnitude and relative signs of the different flavours.

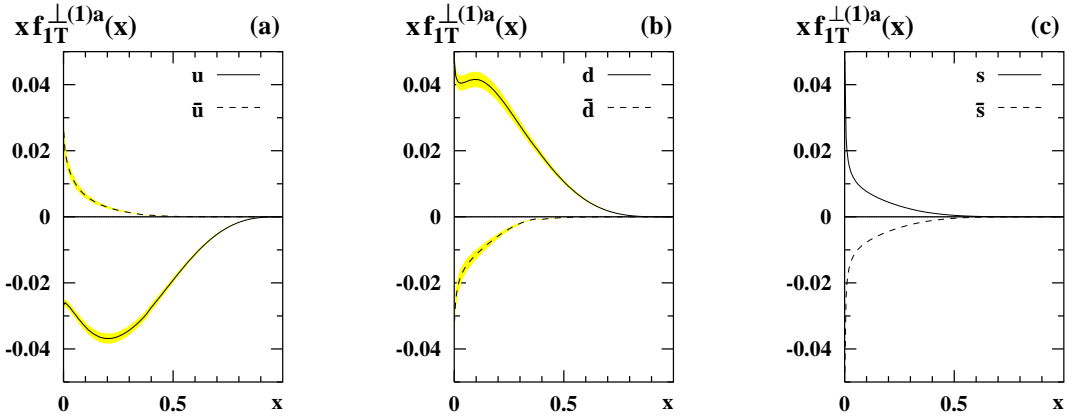


**FIGURE 7.** The  $xf_{1T}^{\perp(1)a}(x)$  vs.  $x$  as extracted from preliminary HERMES and COMPASS data [10, 11]. (a) The flavours  $u$  and  $\bar{u}$ . (b) The flavours  $d$  and  $\bar{d}$ . (c) The flavours  $s$  and  $\bar{s}$  that were fixed to  $\pm$  positivity bounds (17) for reasons explained in Sec. 7, see also Eqs. (18, 19). The shaded areas in (a) and (b) show the respective  $1-\sigma$ -uncertainties.

After these cautious remarks concerning the meaning and interpretation of our results, let us have a look how the obtained Sivers functions look like, see Fig. 7. We make the following observations.

- The Sivers  $u$  and  $d$  distributions are of comparable magnitudes but opposite signs, as predicted in the large- $N_c$  limit [65], see Eq. (16).
- The Sivers  $\bar{u}$  and  $\bar{d}$  distributions are of comparable magnitudes but opposite signs, as predicted in the large- $N_c$  limit [65], see text in the sequence of Eq. (16).
- It is  $2A_u \approx -2A_{\bar{u}} \approx A_d \approx -A_{\bar{d}}$  and  $A_s = -A_{\bar{s}}$ , Eq. (19). Were the former relations exact, then the contribution of  $q, \bar{q}$  ( $q = u, d, s$ ) to the Burkardt sum rule [78, 79]

$$\sum_{a=q,\bar{q},g} \int_0^1 dx f_{1T}^{\perp(1)a}(x) = 0 \quad (20)$$

would vanish, i.e. also  $\int_0^1 dx f_{1T}^{\perp(1)g}(x) = 0$ . That would imply a small Sivers gluon distribution, as concluded independently in [39, 80, 81].<sup>2</sup>

- The Sivers  $u$  and  $d$  distributions obtained here agree qualitatively with earlier works [39, 40, 41, 42, 45] in which sea quarks effects were not considered.
- The signs of the Sivers  $u$  and  $d$  distributions support the picture of Ref. [67].

<sup>2</sup> Notice that strictly speaking the integrals in (20) exist only if  $A_u = -A_{\bar{u}}$  and  $A_d = -A_{\bar{d}}$  holds exactly in the Ansatz (18) (cf. in this context also the model calculation [82] where quark- and gluon Sivers functions cancel under the integral). For  $A_u$  and  $A_{\bar{u}}$  this is the case within  $1-\sigma$ , but for  $A_d$  and  $A_{\bar{d}}$  there is a clearer mismatch, see (19), such that (20) would diverge. However, our parameterization is not meant to be valid for  $x \rightarrow 0$  and is anyway only constraint for  $x > 0.003$  by COMPASS data. We remark that our parameterization also is not meant to be valid for  $x \rightarrow 1$  where the Sivers function is expected to vanish faster than  $f_1^a(x)$  [83].

## 9. PREDICTIONS FOR CLAS AND COMPASS

Fig. 8 shows the predictions, made on the basis of the fit (18, 19), for the  $x$ -dependence of the Sivers SSA of charged pions and kaons from proton targets for two experiments: CLAS with 12 GeV beam upgrade, and COMPASS. The CLAS error projections for 2000 hours run time are from [84, 85]. The COMPASS error projections are estimated assuming a statistics comparable to that of the deuteron target experiment [11].

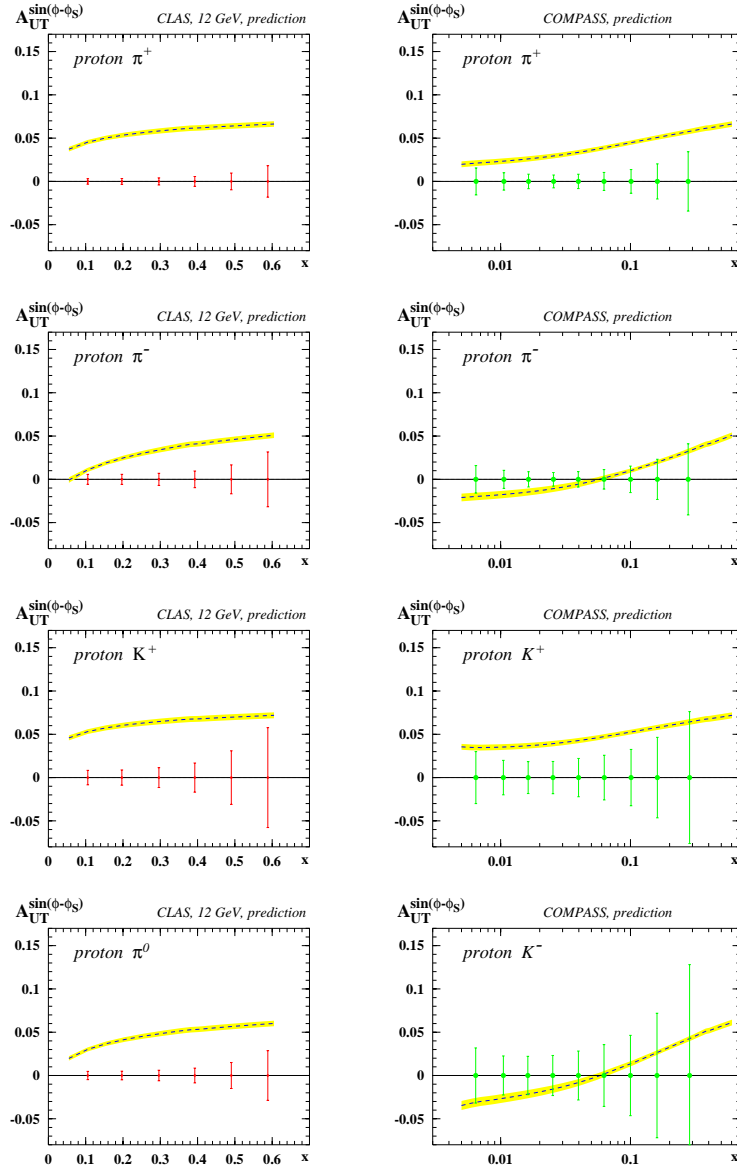


**FIGURE 8.** Predictions for the Sivers SSA as function of  $x$  from a proton target for CLAS at 12 GeV (left panel) and for COMPASS (right panel). The predictions are made on the basis of the fit (18, 19) presented in this work. The CLAS error projections are from [84, 85]. For the COMPASS error estimates we assumed the statistics of [11].

We see that both experiments will be able to confirm (or reject) these predictions within their expected statistical accuracies.

The interesting question is, of course, whether CLAS and COMPASS will confirm the HERMES results for  $K^+$  at  $x \sim 0.15$ , and overshoot our predictions in that region of  $x$ . In this context, however, it is also worth to look more carefully into the kinematics. The next Section is devoted to this task.

## 10. FACTORIZATION AND POWER CORRECTIONS

When averaged over the respectively covered kinematical regions, CLAS, COMPASS and HERMES have a comparable  $\langle Q^2 \rangle \sim (2\text{-}3) \text{ GeV}^2$  (this is what we used in our study). At fixed  $x$ , however,  $Q^2$  can vary significantly in these experiments. For example,

$$\begin{aligned} \text{HERMES: } & \langle x \rangle = 0.115, \quad \langle Q^2 \rangle = 2.62 \text{ GeV}^2, \\ \text{COMPASS: } & \langle x \rangle = 0.1205, \quad \langle Q^2 \rangle = 12.9 \text{ GeV}^2, \end{aligned} \quad (21)$$

which is in the  $x$ -region where the 'trouble' occurs. (At CLAS it is about  $2 \text{ GeV}^2$ .)

Being sure that one really deals with the leading twist contribution, such differences are not dramatic — as long as we are not interested in a high precision study of the effect. But how can we *a priori* be sure that there are no power corrections? Little is known about such corrections to the Sivers effect. For illustrative purposes, let us assume that

$$A_{UT \text{ measured}}^{\sin(\phi - \phi_S)} = \left\{ \text{'twist-2 Sivers effect' in Eqs. (11, 15)} \right\} + C(Q) \frac{M_N^2}{Q^2} \quad (22)$$

as one generically may expect. The 'coefficient'  $C(Q)$  could, in general, be flavour-dependent and typically depend on scale logarithmically (and depend on  $x, z, \dots$  etc.). By looking at (21, 22) we see, that power corrections — if they play a role — are about 5 times smaller at COMPASS compared to HERMES at  $x \sim 0.15$ .

Maybe such corrections are irrelevant for  $Q^2 > 1 \text{ GeV}^2$  which is typically used as DIS-cut. In any case, a careful comparison of all (present and future) data from COMPASS, HERMES and JLab will shed light on the possible size of power corrections.

In particular, data from CLAS (first transverse target data will be available in 2011 [86]) will be valuable — were a wide kinematical range is covered with very high statistics. Moreover, even after the 12 GeV beam energy upgrade, a certain fraction of the beam time also somehow lower beam energies will be available. Therefore, CLAS could provide precise information on SSAs at fixed value of  $x$  but for different  $Q^2$ . Such data would allow to discriminate between 'leading twist' contributions and possible power corrections — paving the way to a concise understanding of the novel effects.

One should not forget that in general 'power corrections' are by no means only 'contaminations' to the parton model formalism. Rather, they also contain interesting physics, we refer to [87] for an example.

## 11. CONCLUSIONS

Since the release of first data on Sivers effect in SIDIS by HERMES and COMPASS [5, 6], more detailed, higher statistics (published and preliminary) data became available [7, 8, 9, 10, 11, 12, 13]. While the first data did not allow to constrain Sivers sea quarks [39, 40, 41, 42, 45], it is clear that the most recent ones [10, 11] can only be described, if the Sivers sea quarks are not zero.

In this work we studied the recent preliminary data [10, 11]. For that we introduced relevant Sivers sea quarks ( $\bar{u}$ ,  $\bar{d}$ ,  $s$ ,  $\bar{s}$ ), and choose a simple Ansatz that assumes the Sivers functions to be proportional to the unpolarized ones. The statistically satisfactory fit provides a good *overall* description of the preliminary data [10, 11].

The resulting Sivers  $u$ ,  $d$ ,  $\bar{u}$ ,  $\bar{d}$  distributions are in excellent agreement with large  $N_c$  predictions [65]. The Sivers  $u$ ,  $d$  distributions confirm earlier analyses [39, 40, 41, 42, 45], and support the physical picture of the Sivers effect from [67]. The fit favors Sivers  $s$ ,  $\bar{s}$  distributions of opposite sign, and close to positivity bounds (in the model-dependent way we implemented them), though this observation has less statistical significance.

That such a fit, that assumes  $f_{1T}^{\perp(1)a}(x) \propto f_1^a(x)$  for all flavours, works implies the following. The present data do not yet give much insights into details of the shapes of the Sivers functions. But they already tell us something about their magnitudes and relative signs, and this situation will improve due to the impact of future data.

One could be happy about this situation. Earlier studies and the optimism, concerning measurability of the Sivers effect in DY, are confirmed [39, 40, 41, 42, 45]. The results fit into theoretical expectations [65, 67]. There is a rough, qualitative agreement with model results [88, 89, 90, 91, 92, 93] especially concerning Sivers quark distributions. But there is also a grain of salt.

The description of the preliminary data [10] on the  $K^+$  Sivers effect around  $x \sim 0.15$  is not ideal. Actually, we speak about 2 out of 61 data points<sup>3</sup> available presently on the Sivers effect in DIS production of various hadrons from various targets. Could these two data points be statistical fluctuations? Should they make us worry? Could they indicate power corrections? Or do they hint at novel effects?

At the present stage it is not possible to draw definite conclusions. Unfortunately, the HERMES experiment is terminated. But fortunately there are promising prospects due to COMPASS with a proton target, and JLab where different transversely and longitudinally polarized targets will be explored [86].

The data from these experiments, which are complementary from the point of view of kinematics, will help to answer these and many other questions — on the Sivers and many other effects [41, 94, 95, 96, 97, 92, 98].

---

<sup>3</sup> We mean here data on  $x$ -dependence from [10, 11] (data on neutral kaons from [13] are not included in this counting). The relevant events, when binned correspondingly, also 'pop up' in data on, for example, the  $z$ -dependence and cause 'mismatches' also there, see Sec. 7. But these are not 'additional mismatches', since the different data sets are correlated.

## ACKNOWLEDGMENTS

We thank the organizers of the “CLAS 12 RICH Detector Workshop” (see <http://conferences.jlab.org/CLAS12/index.html>) for giving us the opportunity to present and discuss our recent work.

We thank Harut Avakian for providing the error projections shown in Fig. 8 and valuable comments on the manuscript. We also thank John Collins, Kyungseon Joo, Andreas Metz, Pavel Pobylitsa and Oleg Teryaev for useful discussions. This work is supported by BMBF (Verbundforschung), COSY-Jülich project, the Transregio Bonn-Bochum-Giessen, and is part of the by EIIIHT project under contract number RII3-CT-2004-506078. A.E. is also supported by RFBR grant 06-02-16215, by RF MSE RNP.2.2.2.2.6546 (MIREA) and by the Heisenberg-Landau Program of JINR.

Notice: Authored by Jefferson Science Associates, LLC under U.S. DOE Contract No. DE-AC05-06OR23177. The U.S. Government retains a non-exclusive, paid-up, irrevocable, world-wide license to publish or reproduce this manuscript for U.S. Government purposes.

## REFERENCES

1. G. Bunce, et al., *Phys. Rev. Lett.* **36**, 1113–1116 (1976).
2. V. D. Apokin, et al., *Sov. J. Nucl. Phys.* **49**, 103 (1989).
3. D. L. Adams, et al., *Phys. Lett.* **B261**, 201–206 (1991).
4. D. L. Adams, et al., *Phys. Lett.* **B264**, 462–466 (1991).
5. A. Airapetian, et al., *Phys. Rev. Lett.* **94**, 012002 (2005), hep-ex/0408013.
6. V. Y. Alexakhin, et al., *Phys. Rev. Lett.* **94**, 202002 (2005), hep-ex/0503002.
7. M. Diefenthaler, *AIP Conf. Proc.* **792**, 933–936 (2005), hep-ex/0507013.
8. E. S. Ageev, et al., *Nucl. Phys.* **B765**, 31–70 (2007), hep-ex/0610068.
9. M. Diefenthaler, *AIP Conf. Proc.* **915**, 509–512 (2007), hep-ex/0612010.
10. M. Diefenthaler (2007), 0706.2242.
11. A. Martin, *Czech. J. Phys.* **56**, F33–F52 (2006), hep-ex/0702002.
12. A. Vossen (2007), 0705.2865.
13. M. Alekseev, et al. (2008), 0802.2160.
14. A. Kotzinian (2007), 0705.2402.
15. A. Airapetian, et al., *Phys. Rev. Lett.* **84**, 4047–4051 (2000), hep-ex/9910062.
16. A. Airapetian, et al., *Phys. Rev.* **D64**, 097101 (2001), hep-ex/0104005.
17. A. Airapetian, et al., *Phys. Lett.* **B562**, 182–192 (2003), hep-ex/0212039.
18. A. Airapetian, et al., *Phys. Lett.* **B622**, 14–22 (2005), hep-ex/0505042.
19. H. Avakian, et al., *Phys. Rev.* **D69**, 112004 (2004), hep-ex/0301005.
20. H. Avakian, P. E. Bosted, V. Burkert, and L. Elouadrhiri, *AIP Conf. Proc.* **792**, 945–948 (2005), nucl-ex/0509032.
21. A. Airapetian, et al., *Phys. Lett.* **B648**, 164–170 (2007), hep-ex/0612059.
22. J. P. Ralston, and D. E. Soper, *Nucl. Phys.* **B152**, 109 (1979).
23. P. J. Mulders, and R. D. Tangerman, *Nucl. Phys.* **B461**, 197–237 (1996), hep-ph/9510301.
24. D. Boer, and P. J. Mulders, *Phys. Rev.* **D57**, 5780–5786 (1998), hep-ph/9711485.
25. A. Bacchetta, M. Diehl, K. Goeke, A. Metz, P. Mulders, and M. Schlegel, *JHEP* **02**, 093 (2007), hep-ph/0611265.
26. X.-d. Ji, J.-p. Ma, and F. Yuan, *Phys. Rev.* **D71**, 034005 (2005), hep-ph/0404183.
27. X.-d. Ji, J.-P. Ma, and F. Yuan, *Phys. Lett.* **B597**, 299–308 (2004), hep-ph/0405085.
28. J. C. Collins, and A. Metz, *Phys. Rev. Lett.* **93**, 252001 (2004), hep-ph/0408249.

29. J. C. Collins, *Nucl. Phys.* **B396**, 161–182 (1993), hep-ph/9208213.
30. D. W. Sivers, *Phys. Rev.* **D41**, 83 (1990).
31. D. W. Sivers, *Phys. Rev.* **D43**, 261–263 (1991).
32. G. A. Miller, *Phys. Rev.* **C76**, 065209 (2007), 0708.2297.
33. S. J. Brodsky, D. S. Hwang, and I. Schmidt, *Phys. Lett.* **B530**, 99–107 (2002), hep-ph/0201296.
34. S. J. Brodsky, D. S. Hwang, and I. Schmidt, *Nucl. Phys.* **B642**, 344–356 (2002), hep-ph/0206259.
35. J. C. Collins, *Phys. Lett.* **B536**, 43–48 (2002), hep-ph/0204004.
36. A. V. Belitsky, X. Ji, and F. Yuan, *Nucl. Phys.* **B656**, 165–198 (2003), hep-ph/0208038.
37. X.-d. Ji, and F. Yuan, *Phys. Lett.* **B543**, 66–72 (2002), hep-ph/0206057.
38. D. Boer, P. J. Mulders, and F. Pijlman, *Nucl. Phys.* **B667**, 201–241 (2003), hep-ph/0303034.
39. A. V. Efremov, K. Goeke, S. Menzel, A. Metz, and P. Schweitzer, *Phys. Lett.* **B612**, 233–244 (2005), hep-ph/0412353.
40. M. Anselmino, et al., *Phys. Rev.* **D72**, 094007 (2005), hep-ph/0507181.
41. W. Vogelsang, and F. Yuan, *Phys. Rev.* **D72**, 054028 (2005), hep-ph/0507266.
42. J. C. Collins, et al., *Phys. Rev.* **D73**, 014021 (2006), hep-ph/0509076.
43. J. C. Collins, et al., *Phys. Rev.* **D73**, 094023 (2006), hep-ph/0511272.
44. J. C. Collins, et al. (2005), hep-ph/0510342.
45. M. Anselmino, et al. (2005), hep-ph/0511017.
46. A. V. Efremov, K. Goeke, and P. Schweitzer, *Czech. J. Phys.* **56**, F181–F194 (2006), hep-ph/0702155.
47. A. V. Efremov, K. Goeke, and P. Schweitzer (2008), 0801.2238.
48. M. Gourdin, *Nucl. Phys.* **B49**, 501–512 (1972).
49. A. Kotzinian, *Nucl. Phys.* **B441**, 234–248 (1995), hep-ph/9412283.
50. M. Diehl, and S. Sapeta, *Eur. Phys. J.* **C41**, 515–533 (2005), hep-ph/0503023.
51. K. Goeke, A. Metz, and M. Schlegel, *Phys. Lett.* **B618**, 90–96 (2005), hep-ph/0504130.
52. M. Anselmino, M. Boglione, and F. Murgia, *Phys. Lett.* **B362**, 164–172 (1995), hep-ph/9503290.
53. U. D’Alesio, and F. Murgia (2007), 0712.4328.
54. A. V. Efremov, and O. V. Teryaev, *Sov. J. Nucl. Phys.* **36**, 140 (1982).
55. A. V. Efremov, and O. V. Teryaev, *Phys. Lett.* **B150**, 383 (1985).
56. J.-w. Qiu, and G. Sterman, *Phys. Rev. Lett.* **67**, 2264–2267 (1991).
57. J.-w. Qiu, and G. Sterman, *Nucl. Phys.* **B378**, 52–78 (1992).
58. J.-w. Qiu, and G. Sterman, *Phys. Rev.* **D59**, 014004 (1999), hep-ph/9806356.
59. C. J. Bomhof, P. J. Mulders, and F. Pijlman, *Phys. Lett.* **B596**, 277–286 (2004), hep-ph/0406099.
60. X. Ji, J.-W. Qiu, W. Vogelsang, and F. Yuan, *Phys. Lett.* **B638**, 178–186 (2006), hep-ph/0604128.
61. P. G. Ratcliffe, and O. V. Teryaev (2007), hep-ph/0703293.
62. J. Collins, and J.-W. Qiu, *Phys. Rev.* **D75**, 114014 (2007), 0705.2141.
63. J. Collins (2007), 0708.4410.
64. I. M. Gregor, *Acta Phys. Polon.* **B36**, 209–215 (2005).
65. P. V. Pobylitsa (2003), hep-ph/0301236.
66. U. D’Alesio, and F. Murgia, *Phys. Rev.* **D70**, 074009 (2004), hep-ph/0408092.
67. M. Burkardt, *Phys. Rev.* **D66**, 114005 (2002), hep-ph/0209179.
68. V. Barone, et al. (2005), hep-ex/0505054.
69. A. Bianconi, and M. Radici, *Phys. Rev.* **D73**, 034018 (2006), hep-ph/0512091.
70. A. Bianconi, and M. Radici, *Phys. Rev.* **D73**, 114002 (2006), hep-ph/0602103.
71. M. Radici, F. Conti, A. Bacchetta, and A. Bianconi (2007), 0708.0232.
72. S. Kretzer, *Phys. Rev.* **D62**, 054001 (2000), hep-ph/0003177.
73. A. Bacchetta, M. Boglione, A. Henneman, and P. J. Mulders, *Phys. Rev. Lett.* **85**, 712–715 (2000), hep-ph/9912490.
74. M. Gluck, E. Reya, and A. Vogt, *Eur. Phys. J.* **C5**, 461–470 (1998), hep-ph/9806404.
75. F. James, *CERN Report 81-03* (1981).
76. J. C. Collins, and J. Pumplin (2001), hep-ph/0106173.
77. S. Melis in collaboration with, M. Anselmino, M. Boglione, A. Kotzinian, A. Prokudin, U. D’Alesio, F. Murgia, and C. Turk, *talk at DIS 2008 in London* (April, 2008).
78. M. Burkardt, *Phys. Rev.* **D69**, 057501 (2004), hep-ph/0311013.
79. M. Burkardt, *Phys. Rev.* **D69**, 091501 (2004), hep-ph/0402014.

80. S. J. Brodsky, and S. Gardner, *Phys. Lett.* **B643**, 22–28 (2006), hep-ph/0608219.
81. M. Anselmino, U. D’Alesio, S. Melis, and F. Murgia, *Phys. Rev.* **D74**, 094011 (2006), hep-ph/0608211.
82. K. Goeke, S. Meissner, A. Metz, and M. Schlegel, *Phys. Lett.* **B637**, 241–244 (2006), hep-ph/0601133.
83. S. J. Brodsky, and F. Yuan, *Phys. Rev.* **D74**, 094018 (2006), hep-ph/0610236.
84. H. Avakian, *private communication* (2008).
85. H. Avakian, et al., *JLab LOI 12-06-108* (2008).
86. H. Avakian, et al., *JLab E-08-015* (2008).
87. J.-P. Chen, A. Deur, and Z.-E. Meziani, *Mod. Phys. Lett.* **A20**, 2745–2766 (2005), nucl-ex/0509007.
88. F. Yuan, *Phys. Lett.* **B575**, 45–54 (2003), hep-ph/0308157.
89. A. Bacchetta, A. Schaefer, and J.-J. Yang, *Phys. Lett.* **B578**, 109–118 (2004), hep-ph/0309246.
90. Z. Lu, and B.-Q. Ma, *Nucl. Phys.* **A741**, 200–214 (2004), hep-ph/0406171.
91. I. O. Cherednikov, U. D’Alesio, N. I. Kochelev, and F. Murgia, *Phys. Lett.* **B642**, 39–47 (2006), hep-ph/0606238.
92. L. P. Gamberg, G. R. Goldstein, and M. Schlegel (2007), arXiv:0708.0324 [hep-ph].
93. A. Courtoy, F. Fratini, S. Scopetta, and V. Vento (2008), 0801.4347.
94. A. V. Efremov, K. Goeke, and P. Schweitzer, *Phys. Rev.* **D73**, 094025 (2006), hep-ph/0603054.
95. M. Anselmino, et al., *Phys. Rev.* **D75**, 054032 (2007), hep-ph/0701006.
96. A. Kotzinian, B. Parsamyan, and A. Prokudin (2006), hep-ph/0603194.
97. H. Avakian, et al., *Phys. Rev.* **D77**, 014023 (2008), 0709.3253.
98. V. Barone, A. Prokudin, and B.-Q. Ma (2008), 0804.3024.